OSIRIS

Optical, Spectroscopic, and Infrared Remote Imaging System

OSIRIS pointing position relative to other boresights on Rosetta

RO-RIS-MPAE-TN-051
Issue: 1
Revision: g
23 June 2020

Prepared by:
Cecilia Tubiana

Approval Sheet

Cecilia Tubiana Digitally signed by Cecilia Tubiana Date: 2020.07.10 20:46:23 +02'00'

Prepared by: *C. Tubiana* (signature/date)

Digitally signed by Carsten Güttler
Date: 2020.07.13 10:46:32 +02'00'

Approved by: *H. Sierks* (signature/date)

Document Change Record

Iss./Rev.	Date	Author	Pages affected	Description
1/-	27/04/2005	M. Küppers	all	first release
1/a	30/11/ 2006	M. Küppers	5,8	Update Version number of relevant ESA document. Update Table 1 following RSOC update.
1/b	23/01/2007	M. Küppers	5,8	Adjusted VIRTIS H boresight following new boresight determination.
1/c	1/06/2007	M. Küppers	5,8	Again adjustment of VIRTIS H boresight.
1/d	18/01/2008	M. Küppers	5,8	Changes for VIRTIS H and the ALICE wide slits.
1/e	4/12/2017	C. Tubiana	all	Modified Section 2: (a) added CCD coordinate frame, (b) replaced figures with NAC/WAC view in standard Rosetta orientation, (c) added Rosetta coordinate frame. Replaced CAMERA coordinates with CCD coordinates throughout the document. Corrected S/C axis in Section 3. Improved explanation in header of Table 2.
1/f	10/12/2019	X. Shi	5, 8-10	Modified Section 1.4: added RD2. Modified Section 3: updated parameters in Table 1 and text accordingly. Added Section 4 on the update of WAC boresight parameters.
1/g	23/06/2020	X. Shi C. Güttler	6, 8-13	Corrected typo in section 2.2 Added section 2.4 on definition of OSIRIS frames Modified section 3 based on latest boresight parameters Modified section 4 to include details of latest boresight analysis

Table of contents

1 General aspects

1.1 Scope

This document provides the offsets between the Rosetta spacecraft $Z_{S/C}$ axis and the boresights of the different remote sensing instruments. It also provides the position of the pointing target in the OSIRIS field of view for each boresight.

1.2 Introduction

On Rosetta there are 5 remote sensing instruments: Alice, MIRO, NavCams, OSIRIS, and VIRTIS. The boresights of the instruments differ by tens of arcminutes. For a given observations, the spacecraft can only point to one boresight. This document defines the coordinate systems involved and predicts the target position on the OSIRIS cameras for the different boresights.

1.3 Applicable Documents

No.	Document Name	Document Number (actual Iss./Rev.)

1.4 Reference Documents

No.	Document Name	Document Number (actual Iss./Rev.)
RD1	ROSETTA Payload Boresight Alignment Details	RO-EST-TN-3305 2/g
RD2	Rosetta SPICE frame kernel	ROS_V36.TF
RD3	OSIRIS camera distortion and boresight correction	RO-RIS-MPAE-TN-081 GEOMETRIC_DIST_COR_V??.PDF
RD4	OSIRIS Georeferenced Data Products	RO-RIS-MPAE-TN-089 GEO_PRODUCTS_V??.PDF

2 Coordinate frames

There are a number of coordinate systems relevant to the interpretation of OSIRIS data. These coordinate systems can be separated into two groups: (a) pixel coordinate systems referring directly to the CCD and (b) inertial coordinate systems referring to the spacecraft and viewing geometry.

2.1 OSIRIS CCD coordinate frame

Figure 1 shows the OSIRIS NAC and WAC CCD array.
In the CCD coordinate frame, pixel (0, 0) is always the closest pixel to amplifier A, independently from which amplifier is used to read-out the image.

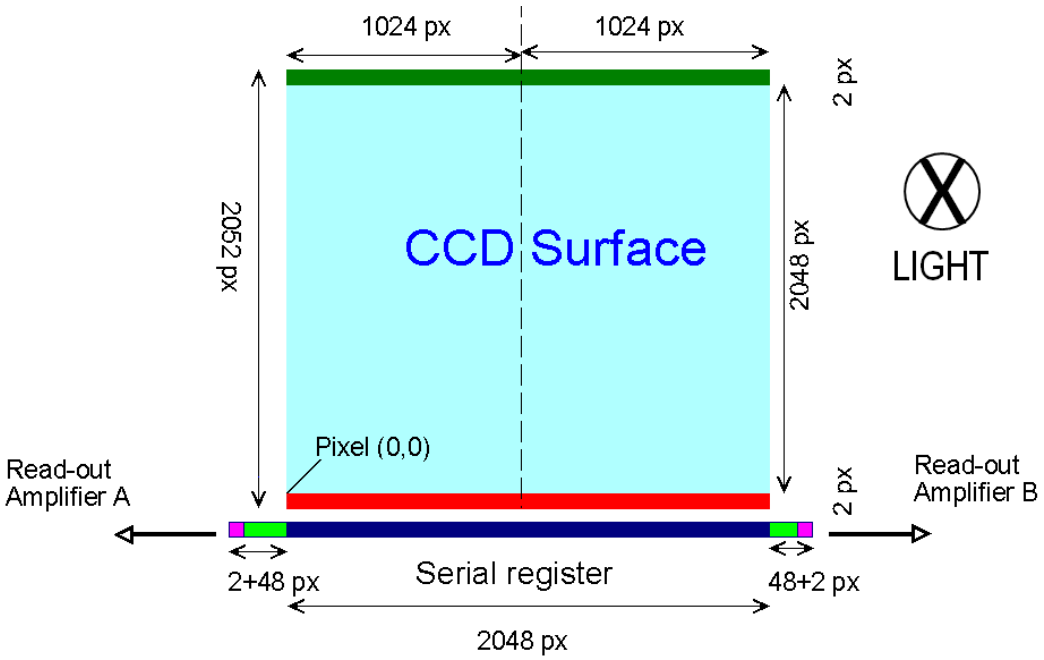

Figure 1 CCD array as seen by the light beam.

The first pixel to be read-out is the closest to the used amplifier. The on board software re-arranges each line as if the CCD would have been read out through amplifier A. In this way, the first pixel in the image corresponds always to pixel (0, 0).
Lines are parallel to the serial register. The *line numbers* increase with distance from the serial register. Samples are perpendicular to the serial register. The *sample numbers* increase with distance from the edge of the CCD that contains read-out amplifier A.

2.2 Standard Rosetta orientation

To display OSIRIS images in the "standard Rosetta orientation" as most of the Rosetta products and tools (NAVCAM, 3DTool, MAPPS):

- WAC images have pixel (0,0) in the bottom right corner, the line number increases from bottom to top and the sample number increases from right to left (Figure 2, left).
- NAC images have pixel (0,0) in the bottom left corner, the line number increases from bottom to top and the sample number increases from left to right (Figure 2, right).

The direction in which the line number and the sample number increase is stored in the PDS header keywords LINE_DISPLAY_DIRECTION and SAMPLE_DISPLAY_DIRECTION, respectively. To display the images in the standard Rosetta orientation, an additional 180° rotation has to be applied to both NAC and WAC images.

Figure 2 shows the NAC and the WAC images in the standard Rosetta orientation. In this orientation, the spacecraft $+X_{S/C}$ axis is up and the spacecraft $+Y_{S/C}$ axis to the right, meaning that the Sun is up in most images.

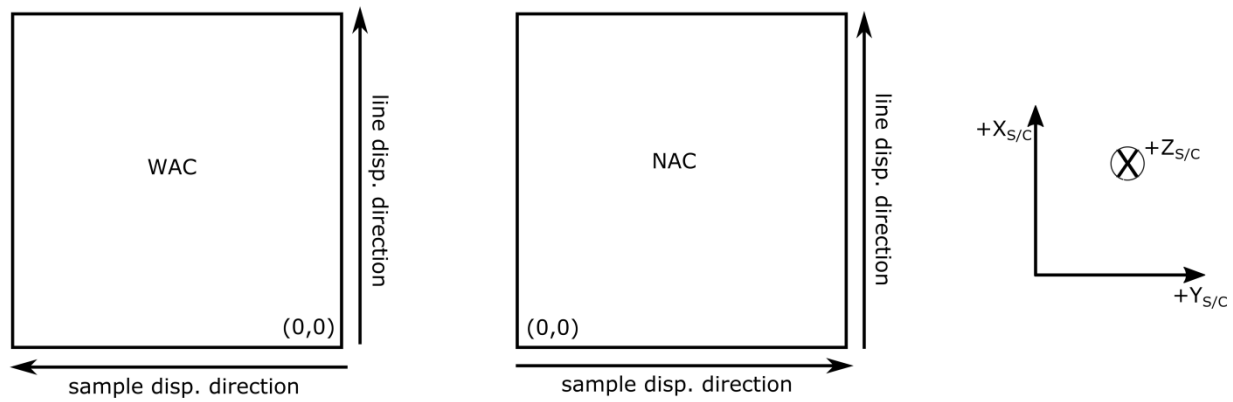

Figure 2 WAC and NAC images in the standard Rosetta orientation.

2.3 Rosetta spacecraft coordinate frame

In the Rosetta spacecraft coordinate frame:

- the $+Z_{S/C}$ axis is aligned with the direction of nominal pointing of remote sensing instruments (orthogonal to the payload plane)
- the $+Y_{S/C}$ axis is oriented along the solar panels
- the $+X_{S/C}$ is orthogonal to the high gain antenna mounting panel.

The Rosetta spacecraft coordinate frame can be addressed in the SPICE system using the coordinate frame alias “ROS_SPACECRAFT”.

2.4 OSIRIS coordinate frames

The OSIRIS cameras are mounted on the $-X_{S/C}$ panel of the spacecraft. Nominally, OSIRIS camera frames are co-aligned with the s/c frame. The remaining misalignment is specified with three angles:

- Offset from Z s/c: x: the angle between the projection of the boresight onto the s/c XZ plane and the +Zs/c axis, measured positive from the +Zs/c toward the +Xs/c axis.
- Offset from Z s/c: y: the angle between the projection of the boresight onto the s/c YZ plane and the +Zs/c axis, measured positive from the +Zs/c toward the +Ys/c axis.
- Rotation around Z s/c: the angle of rotation of the camera frame around the s/c +Z axis, measured positive counter clockwise.

To accommodate different types of observations, two sets of OSIRIS frames are defined in SPICE:

- 67P frames: frames for observations targeted at the nucleus of comet 67P, named as “ROS_OSIRIS_NAC_67P” and “ROS_OSIRIS_WAC_67P” for NAC and WAC, respectively.

- Non-67P frames: frames for other observations, named as "ROS_OSIRIS_NAC_NON_67P" and "ROS_OSIRIS_WAC_NON_67P" for NAC and WAC, respectively.

Latest values used for defining the orientation of different OSIRIS frames are summarized in Table 1, which are implemented in RD2. The determination procedure of frame parameters is detailed in section 4.

Frame name	**$X_{S/C}$ offset from $+Z_{S/C}$ axis [deg]**	**$Y_{S/C}$ offset from $+Z_{S/C}$ axis [deg]**	**Rotation around $+Z_{S/C}$ axis [deg]**
ROS_OSIRIS_NAC_67P	-0.0313	0.0108	-0.218
ROS_OSIRIS_WAC_67P	0.374	0.0736	0.113
ROS_OSIRIS_NAC_NON_67P	-0.0363	0.0179	-0.218
ROS_OSIRIS_WAC_NON_67P	0.369	0.0807	0.113

Table 1 Parameters of OSIRIS frames as implemented in RD2.

3 Boresight offsets and CCD pixel positions of boresights

The definition of various Rosetta boresights as well as their relative positions are documented in RD1. Parameters used for boresight definitions are being updated over time and recorded in Rosetta SPICE frame kernel. Table 2 summarizes boresight parameters used at the time of this document, as described in RD2 and references therein. 67P frames are used here as the reference OSIRIS frames. Positions of boresights relative to the non-67P OSIRIS frames can be derived in a similar manner.

Boresight	($X_{S/C}$, $Y_{S/C}$) offset from $+Z_{S/C}$ axis [deg]	X,Y position of boresight on NAC (CCD coordinates)[1]	X,Y position of boresight on WAC (CCD coordinates)[2]
$Z_{S/C}$ axis	0.0, 0.0	1014.1, 1053.1	1036.8, 958.4
ALICE narrow center	0.062323, -0.106796	915.3, 1111.2	1055.5, 969.3
ALICE –X wide top	1.9955, -0.11344	Outside FOV	1057.8, 592.4
ALICE +X wide bottom	-1.91656, -0.12593	Outside FOV	1061.8, 1312.4
MIRO sub-mm	-0.082, -0.0067	1007.6, 977.0	1037.9, 944.0
MIRO mm	-0.018, -0.057	961.2, 1036.6	1046.8, 955.2
NAC_67P	-0.0313, 0.0108	1024.0, 1024.0	1034.9, 952.9
WAC_67P	0.374, 0.0736	1083.7, 1399.6	1024.0, 1024.0
VIRTIS-M_VIS_ZERO	-0.071620, 0.032945	1044.4, 986.5	1031.0, 945.8
VIRTIS-M_IR_ZERO	-0.071620, -0.025926	989.8, 986.7	1041.3, 945.8
VIRTIS-H	-0.0936, 0.0027	1016.3, 966.3	1036.3, 942.0
NAVCAM 1	-0.033469, -0.179234	847.8, 1022.7	1068.2, 952.4
NAVCAM 2	0.006631, 0.120223	1125.6, 1058.8	1015.7, 959.6
AL-MR co-operation	-0.082, -0.098	923, 977	1053.8, 945.4

Table 2 Configuration of Rosetta instrument boresights and their positions on the CCDs of OSIRIS cameras relative to OSIRIS frames "ROS_OSIRIS_NAC_67P" and "ROS_OSIRIS_WAC_67P". The second column lists the offset of each instrument boresight from the spacecraft $+Z_{S/C}$ axis. ($X_{S/C}$, $Y_{S/C}$): the first of the two angles is the angle between the projection of the boresight onto the S/C XZ plane and the $+Z_{S/C}$ axis, measured positive from the $+Z_{S/C}$ toward the $+X_{S/C}$ axis. The second of the two angles is the angle between the projection of the boresight onto the S/C YZ plane and the $+Z_{S/C}$ axis, measured positive from the $+Z_{S/C}$ toward the $+Y_{S/C}$ axis. The third and fourth columns

[1] Same as standard Rosetta orientation for NAC.

[2] Horizontally flipped wrt. standard Rosetta orientation for WAC.

list the expected pixel position of the boresight on distortion-corrected CCD planes of NAC and WAC, respectively. Pixel position (1024.0, 1024.0) refers to the center of the CCD, which is at the corners between four pixels.

4 Determination of OSIRIS frames

In view of possible variations in OSIRIS boresights during the mission, an effort was initiated in 2017 to update boresight parameters for both cameras.

4.1 WAC boresight parameters from December 2019

A calibration of the WAC boresight relative to that of NAC was done in December 2019, based on analysis of OSIRIS star calibration sequences (as listed in Table 3).

Star images taken by both WAC and NAC cameras within a relatively short time span are used for the calibration. For each image, CCD positions of selected stars in the field of view are measured by Point Spread Function fitting. The pointing of the camera in the inertial frame is then estimated by fitting predicted CCD positions of stars to their measurements. Assuming that the spacecraft attitude stays unchanged during the time, the offset between WAC and NAC boresights can be derived by direct comparisons between pointing of WAC and NAC observations. As a result, a time series of the boresight offset between the two OSIRIS cameras are derived.

The updated WAC boresight parameters are calculated by adding the median value of the WAC-to-NAC boresight offset to the NAC boresight parameters. The updated WAC boresight has offset angles of (0.372°,0.074°) relative to the Rosetta spacecraft +Z axis. These values are implemented in the Rosetta SPICE frame kernel ROS_V35.TF.

No.	Sequence Name	Image Name
1	STP003_CALIB_FIELD_NAC	NAC_2014-05-11T04.01.04.144Z_ID10_1397549000_F82 NAC_2014-05-11T03.43.31.207Z_ID10_1397549000_F27 NAC_2014-05-11T03.46.11.207Z_ID10_1397549000_F22
	STP003_CALIB_FIELD_WAC	WAC_2014-05-11T06.00.38.431Z_ID10_1397549000_F12 WAC_2014-05-11T06.01.55.412Z_ID10_1397549000_F21
2	STP003_CALIB_ZETA_OPH_ALICE	WAC_2014-05-12T09.53.26.836Z_ID10_1397549000_F12 WAC_2014-05-12T09.57.17.979Z_ID10_1397549000_F21 NAC_2014-05-12T09.51.32.789Z_ID10_1397549000_F27 NAC_2014-05-12T09.50.08.689Z_ID10_1397549000_F22
3	STP003_CALIB_STARS_001	WAC_2014-05-18T09.02.37.224Z_ID10_1397549000_F12 WAC_2014-05-18T09.02.42.145Z_ID10_1397549000_F21 WAC_2014-05-18T09.01.55.634Z_ID10_1397549000_F18 NAC_2014-05-18T09.09.39.393Z_ID10_1397549000_F41 NAC_2014-05-18T09.08.15.328Z_ID10_1397549000_F27 NAC_2014-05-18T09.10.04.653Z_ID10_1397549000_F82 NAC_2014-05-18T09.09.34.388Z_ID10_1397549000_F22
4	STP043_VEGA_001	WAC_2015-02-11T18.15.42.148Z_ID10_1397549006_F12 WAC_2015-02-11T18.15.49.990Z_ID10_1397549007_F21 NAC_2015-02-11T18.15.08.368Z_ID10_1397549003_F41 NAC_2015-02-11T18.14.57.108Z_ID10_1397549002_F27 NAC_2015-02-11T18.15.53.878Z_ID10_1397549007_F82
5	STP069_VEGA_001	WAC_2015-08-14T14.50.36.577Z_ID10_1397549006_F12 WAC_2015-08-14T14.50.44.353Z_ID10_1397549007_F21 NAC_2015-08-14T14.50.02.614Z_ID10_1397549003_F41 NAC_2015-08-14T14.51.24.502Z_ID10_1397549010_F87 NAC_2015-08-14T14.49.51.155Z_ID10_1397549002_F27

6	STP075_VEGA_001	WAC_2015-09-28T04.37.13.504Z_ID10_1397549006_F12 WAC_2015-09-28T04.37.21.364Z_ID10_1397549007_F21 NAC_2015-09-28T04.37.48.548Z_ID10_1397549009_F27 NAC_2015-09-28T04.36.03.585Z_ID10_1397549000_F41 NAC_2015-09-28T04.36.50.285Z_ID10_1397549004_F82
7	STP085_VEGA_002	WAC_2015-12-08T21.20.03.008Z_ID10_1397549006_F12 WAC_2015-12-08T21.20.12.572Z_ID10_1397549007_F21 NAC_2015-12-08T21.20.29.456Z_ID10_1397549009_F27 NAC_2015-12-08T21.18.44.765Z_ID10_1397549000_F41 NAC_2015-12-08T21.19.31.054Z_ID10_1397549004_F82
8	STP089_VEGA_001	NAC_2015-12-31T20.31.20.270Z_ID10_1397549009_F27 WAC_2015-12-31T20.30.30.312Z_ID10_1397549006_F12 WAC_2015-12-31T20.30.39.412Z_ID10_1397549007_F21 NAC_2015-12-31T20.30.21.480Z_ID10_1397549004_F82

Table 3 OSIRIS observation sequences and images used for updating WAC boresight parameters.

4.2 Frame parameters from June 2020

A new set of boresight parameters is determined for both cameras by June 2020. The analysis utilizes star observations carried out through the Rosetta mission, including most of the Vega observations, some of the ZetaCas observations, and several star field observations (listed in Table 12 of RD3). By minimizing measured and predicted star positions on camera CCD, values of the three angles for defining OSIRIS frames were estimated. They are implemented as non-67P OSIRIS frames "ROS_OSIRIS_NAC_NON_67P" and "ROS_OSIRIS_WAC_NON_67P" for NAC and WAC, respectively.

A different set of parameters was derived for observations targeted at the nucleus of 67P. The method is based on computing shifts between OSIRIS Level 3 (CODMAC L4) images and simulated images. This is done with a 2D correlation between these two images, which can be interpreted as a spacecraft or boresight rotation under the assumption that the spacecraft position is correct. The method is described in more detail in [RD4]. For the purpose of computing a boresight that is in average best matching observations of 67P, a representative set of 1201 NAC and 144 WAC images from color sequences using all color filters and spanning over the whole mission was used. The shifts were computed for each image, the results were filtered for goodness as described in [RD4] and then the resulting 2D correlation results (Figure 3, right, in [RD4]) were stacked. The result is presented in Figure 3.

The instrument frame kernel that was used for the simulated images in this computation was based on ROS_V35.TF, modified for the rotation around the spacecraft *z*-axis as described above. The residual shift is (2, -4) pixels for the NAC in the coordinate system of Figure 3, displayed in the Rosetta Standard Orientation. This shift was compensated in a modified instrument frame by changing "Offset from Z s/c: x" and "Offset from Z s/c: y" as defined in section 2.4. The resulting frames are called "ROS_OSIRIS_NAC_67P" and "ROS_OSIRIS_WAC_67P".

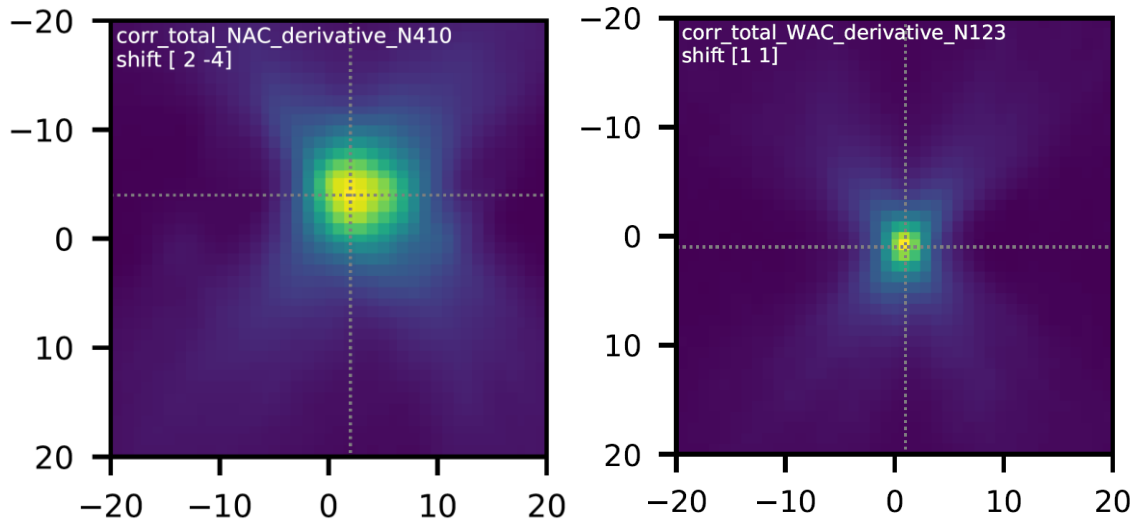

Figure 3 Resulting stack of 2D correlations for the NAC (left) and WAC (right), showing the mismatch of ROS_OSIRIS_NAC / ROS_OSIRIS_WAC in ROS_V35.TF.